Phase diagram and edge states of the ν=5/2 fractional quantum Hall state with Landau level mixing and finite well thickness

Anthony Tylan-Tyler and Yuli Lyanda-Geller

Phys. Rev. B **91**, 205404 — Published 8 May 2015

DOI: 10.1103/PhysRevB.91.205404

Phase diagram and edge states of the $\nu = 5/2$ fractional quantum Hall state with Landau level mixing and finite well thickness

Anthony Tylan-Tyler[1] and Yuli Lyanda-Geller[1,2]

[1] *Department of Physics and Astronomy, Purdue University, West Lafayette, Indiana 47907, USA*
[2] *Birck Nanotechnology Center, Purdue University, West Lafayette, Indiana 47907, USA*

The $\nu = 5/2$ fractional quantum Hall effect is a system of intense experimental and theoretical interest as its ground state may host non-abelian excitations, but the exact nature of the ground state is still undetermined. We present the results of an exact diagonalization study of an electron system in the disk configuration including the effects of Landau level (LL) mixing and the finite thickness of the quantum well confining the electrons. The degeneracy between the two leading candidates for the ground state, the Pfaffian and anti-Pfaffian, is broken by interactions with a neutralizing background, in addition to the inclusion of two- and three-body interactions via LL mixing. As a result of the neutralizing background in the disc configuration, there is a phase transition from the anti-Pfaffian to the Pfaffian as LL mixing is turned on, in stark contrast to what is observed in a spherical geometry. This behavior is in agreement with existing experiment, showing the appearence of the Pfaffian state at strong LL mixing before the system enters a compressible phase. The inclusion of LL mixing leads to an increased charge $e/4$ quasihole size. LL mixing interactions are also shown to overcome the effects of edge reconstruction. Due to finite thickness effects, these properties are enhanced dramatically. We also find that only the Pfaffian and anti-Pfaffian states continue to possess energy gaps at finite width, while gaps for compressible stripe states close, which is in agreement with available experimental data.

I. INTRODUCTION

The $\nu = 5/2$ fractional quantum Hall effect (FQHE)[1,2] is a unique state as it is the only even-denominator FQHE state observed. As a result of the even denominator fractional filling, it cannot be modeled using the Laughlin[3] or the non-interacting composite fermion[4] pictures, which have successfully described the odd denominator states in the lowest Landau level. This has led to the state being considered a paired state of composite fermions[5] which naturally led to the Moore-Read Pfaffian trial state[6–8]. Since the Pfaffian is not particle-hole symmetric, we must also consider the particle-hole conjugate state, the anti-Pfaffian[9,10] as a trial ground state.

These states in particular attract the most theoretical and experimental interest as they may host non-abelian quasihole excitations[6,11–14]. With such excitations, these states may be used to perform topologically protected quantum computing[15,16]. In order to be able to take advantage of this topological protection, it is necessary to determine which trial ground state is realized in experiment. This, in turn, requires including particle-hole symmetry breaking terms into theoretical models, lifting the degeneracy between the Pfaffian and the anti-Pfaffian.

There is evidence that this symmetry is spontaneously broken[17], but there are effects in the system, which break the particle-hole symmetry of the Hamiltonian, such as Landau level (LL) mixing. LL mixing breaks this symmetry through effective three-body potentials which have been calculated using a diagrammatic expansion of the Coulomb interaction[18–22]. In addition to offering particle-hole symmetry breaking, the inclusion of the three-body terms brings the model systems closer to the ideal three-body Hamiltonian, for which the Pfaffian is the state with the lowest energy and angular momentum[7,8]. Many recent exact diagonalization studies in the half-filled first excited LL spherical geometry have included such LL mixing terms[23–26], and a density matrix renormalization group study on the cylinder includes LL mixing by allowing occupation of the second excited LL and lowest LL neighboring the half-filled first excited LL[27]. The most recent exact diagonalization study in a spherical geometry in Ref. 26 additionally includes finite thickness of the quantum well, which has previously been noted to improve overlaps with the Pfaffian state[28–30].

These studies have been somewhat contradictory in their findings. The exact diagonalization study conducted in Ref. 26 shows that the Pfaffian state is favored at lower LL mixing strength and may transition into the anti-Pfaffian state as the LL mixing is turned on. The infinite density matrix renormalization calculation in Ref. 27, however, favors the anti-Pfaffian in the weak LL mixing limit.

In order to further examine the problem and possibly resolve the discrepancy, we present the results of an exact diagonalization study on the disk. Our model system includes interactions with a neutralizing background which provides additional particle-hole symmetry breaking. From this model, we produce a phase diagram of the first excited LL by varying LL mixing strength and varying the distance between the two-dimensional electron gas (2DEG) and the neutralizing background. This shows a transition from the anti-Pfaffian to the Pfaffian as LL mixing is turned on, the opposite of the transition found in Ref. 26, where the Pfaffian transitions into the anti-Pfaffian as the LL mixing is turned on. We then explore the quasihole excitations of the system. Our results show that the inlcusion of LL mixing leads to a larger quasihole, as proposed in Ref. 34. Furthermore,

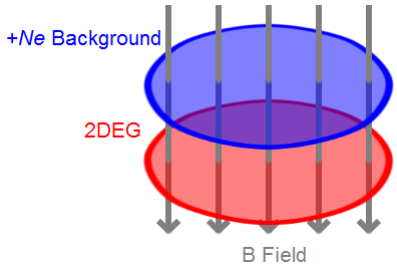

FIG. 1. Our system consists of a 2DEG of width w separated from a disk of neutralizing background charge by a distance d in a perpendicular magnetic field B.

we find that the finite thickness of the system leads to an increase in the quasihole size as well. Finally we use overlaps integrals to find the edge states of the system and examine their behavior as LL mixing and finite thickness is included. The LL mixing is seen to prevent the effects of edge reconstruction[35] from occurring while the finite thickness is seen to generally improve the edge states.

Our paper is organized as follows. In Sec. II we describe our model and discuss particle-hole symmetry breaking. The phase diagram of the system and the transition from the anti-Pfaffian to the Pfaffian is discussed in Sec. III. The quasihole excitations of the system are described in Sec. IV, and the edge states are discussed in Sec. V We conclude with a discussion of the results in Sec. VI.

II. MODEL

We are interested in a system consisting of a 2DEG confined by a disk of neutralizing charge subjected to a perpendicular magnetic field, as illustrated in Fig. 1. As we are including LL mixing through the perturbative expansion of the Coulomb interaction, we can vary both the distance to the neutralizing background and the strength of the LL mixing terms. By varying both of these parameters, we can produce a phase diagram of the system as a function of LL mixing and the strength of the neutralizing background. Furthermore, we include finite thickness effects into our system, which we do for an infinite rectangular well potential. In the following, we choose to express all lengths in units of the magnetic length $\ell_B = \sqrt{c\hbar/eB}$ and energies in units of the Coulomb energy $e^2/\epsilon\ell_B$.

Due to the disk geometry of our system we work in the symmetric gauge. The single particle eigenstates, in cylindrical coordinates, then take the form

$$\psi_{n,m}(r,\theta,z) = \sqrt{\frac{n!}{2\pi(m+n)!}}\left(\frac{r}{\sqrt{2}}\right)^m e^{im\theta}e^{\frac{-r^2}{4}} \times L_n^m\left(\frac{r^2}{2}\right)\sqrt{\frac{1}{w}}\sin\frac{\pi z}{w} \quad (1)$$

when we restrict the system to the lowest lying subband. The angular momentum of the single electron state is then given by m, n is the LL index, and w is the width of the rectangular potential well confining the 2DEG. In the limit of $w \to 0$, we have $\sqrt{1/w}\sin\pi z/w \to 1$, recovering the results for a strictly two-dimensional system.

We include the single particle interactions with the disk by using the potentials

$$U_m(d,w) = \frac{-N}{\pi R_d^2}\int_0^{R_d}\int_0^{2\pi} RdRd\phi\langle 1,m|(r^2+R^2 - 2rR\cos(\theta-\phi)+(z-d)^2)^{-1/2}|1,m\rangle \quad (2)$$

where R_d is the radius of the disk, N is the number of particles, and $\psi_{n,m}(r,\theta,z) = \langle r,\theta,z|n,m\rangle$. By choosing an appropriate R_d, we can control the filling factor of our disk[31,32] and so we fix R_d such that we have a constant filling factor of $1/2$ for the partially filled LL. This background interaction term is the only contribution to the single particle Hamiltonian as the kinetic energy of the system is quantized by the B field. Thus, the single particle term takes the form

$$H_1(d,w) = \sum_m U_m(d,w)a_m^\dagger a_m \quad (3)$$

where the $a_m^{(\dagger)}$ annihilate (create) an electron in the first excited LL with angular momentum m. By introducing an energy cost for the electrons to occupy the edge of the system, this potential contributes to breaking the particle-hole symmetry[32].

The interaction terms can then be classified into two parts, the two-body interactions and the three-body interactions. The two-body Hamiltonian is given by

$$H_2(\kappa,w) = \frac{1}{2}\sum_{k,l,m} V_{l,m}^k(w)a_{m+k}^\dagger a_{l-k}^\dagger a_l a_m + \kappa\sum_{i<j}\sum_M V_M^{(2)}(w)P_{(i,j)}^M. \quad (4)$$

where $\kappa = e^2/\epsilon\ell_B\hbar\omega_B$ is a parameter characterizing the strength of LL mixing, $V_M^{(2)}$ are the Haldane pseudopotentials[36] for the second order two-body corrections as described in Ref. 20, and $P_{(i,j)}^M$ project the state of electrons i and j onto the relative angular momentum state[37] with relative angular momentum M. The remaining term describes the lowest order Coulomb correction and is given by

$$V_{l,m}^k(w) = \left\langle 1,m+k;1,l-k\left|\frac{1}{r_{12}}\right|1,m;1,l\right\rangle. \quad (5)$$

The three-body term is then given by

$$H_3(\kappa,w) = \kappa\sum_{i<j<k} V_M^{(3)}(w)P_{i,j,k}^M \quad (6)$$

where $V_M^{(3)}$ are the three-body Haldane pseudopotentials and $P_{i,j,k}^M$ is a three-body projection operator similar to the one described for the two-body term.

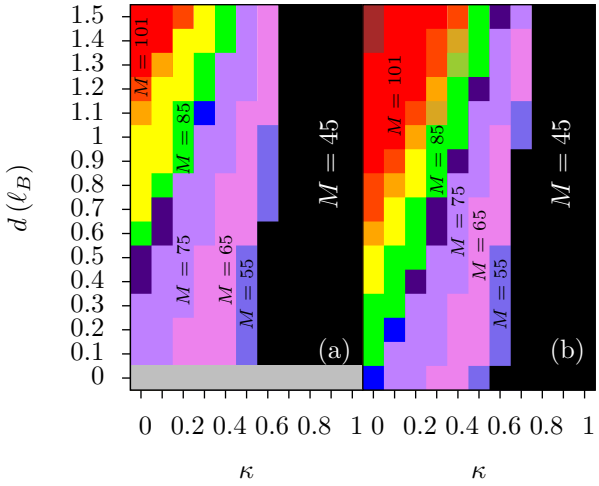

FIG. 2. (a) The phase diagram of 10 electrons in 18 states with $w = 0\ell_B$ as the distance to the neutralizing disk d and the LL mixing strength κ are varied. (b) The phase diagram for varying d and κ with $w = 1\ell_B$. The potential Pfaffian region is highlighted in green for both diagrams while the anti-Pfaffian is highlighted in red. The inclusion of the effect of the finite well thickness expands both of these regions.

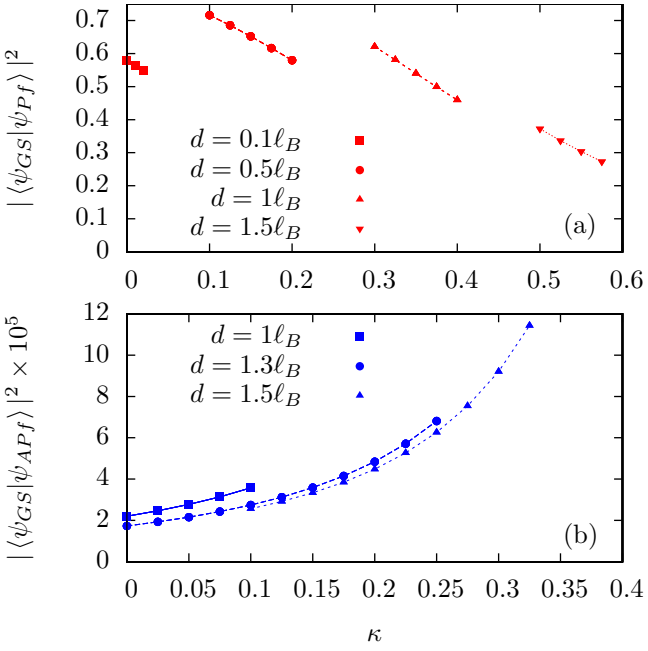

FIG. 3. (a) The overlap integral with the MR Pfaffian at various d. It is apparent that the overlap increases with increasing d and κ until a critical separation, at which point the overlap begins to decrease. (b) The overlap integral with the anti-Pfaffian at various d. The overlap is seen to sharply increase with increasing κ and d.

Combining these three terms, we then have

$$H(\kappa, d, w) = H_1(d, w) + H_2(\kappa, w) + H_3(\kappa, w). \quad (7)$$

This Hamiltonian describes our system and gives us three parameters which can be varied: the distance to the neutralizing background, d, the width of the quantum well, w, and the LL mixing strength, κ.

III. PHASE DIAGRAM

We diagonalize Eq. (7) by breaking up the Hilbert space into subspaces of fixed angular momentum which are diagonalized individually as the rotational invariance causes these subspaces to decouple from each other[32]. The lowest energy state of each subspace is then found and we consider the state with the lowest global energy to be the ground state at that d, w, and κ. We use the total angular momentum of the Pfaffian, $N(2N-3)/2$ where N is the number of electrons, and of the anti-Pfaffian, $S(S-1)/2-(S-N)[2(S-N)-3]/2$ where S is the number of available states, to identify regions where these states may be realized. Performing this process for multiple values of d, w and κ, we are able to produce a phase diagram of the system.

The results of this procedure are shown in Fig.2 for 10 electrons in 18 states with $w = 0\ell_B$ and $w = 1\ell_B$. The noticeable effect of the LL mixing is that all of the observed states arise at larger d than in the absence of mixing. Thus, the LL mixing strength and the confinement by the neutralizing disk, due to the generally attractive nature of the LL mixing terms, balances with the Coulomb repulsion. As d increases, the confinement of the 2DEG by the neutralizing background weakens and the Coulomb interaction pushes the 2DEG towards the edge, while the LL mixing interaction can pull the electrons back to the center as it is increased. Thus, from the model, larger d correspond to larger κ.

Due to the small size of our system, we characterize it by a neutralizing disk of radius $\sim 6\ell_B$. Therefore we do not exceed $d = 1.5\ell_B$ in order to maintain a charge distribution similar to experiment, as in previous simulations of the FQHE on the disk[32]. Realistic experimental separations are significantly larger, being closer to $\sim 10\ell_B$. As larger d leads to weaker confinement by the neutralizing background, the corresponding κ must be increased to compensate and realize the same state as we observe at lower d. Thus, we expect larger values of κ in experimental settings due to the larger characteristic d. Therefore, both d and κ are vital for the realization of the non-abelian states in experimentally relevant ranges of disk separations and LL mixing strength.

This balancing is highlighted in Fig 3a where we see that the overlap with the Pfaffian, which occupies the $M = 85$ region in Fig. 2, increases with increasing d and κ up to some $d_c \simeq 0.5\ell_B$ when $w = 1\ell_B$ and $d_c \simeq 1.2\ell_b$ for $w = 0\ell_B$. This d_c is a finite size effect arising from the distance between the disk and the 2DEG in combination with the finite thickness becoming comparable to the radius of the disk. From Fig. 3a, we can also see

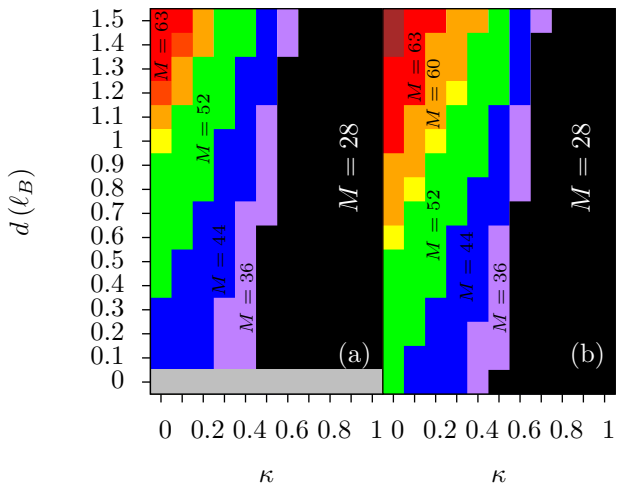

FIG. 4. (a) The phase diagram for 8 electrons in 14 states with $w = 0\ell_B$ as d and κ are varied. (b) The phase diagram for 8 electron in 14 states with $w = 1\ell_B$. We note that in the 8-electron case, the anti-Pfaffian state does not appear and that the size of the collapsed region and the Pfaffian regions decrease in size when we move to 10 particles.

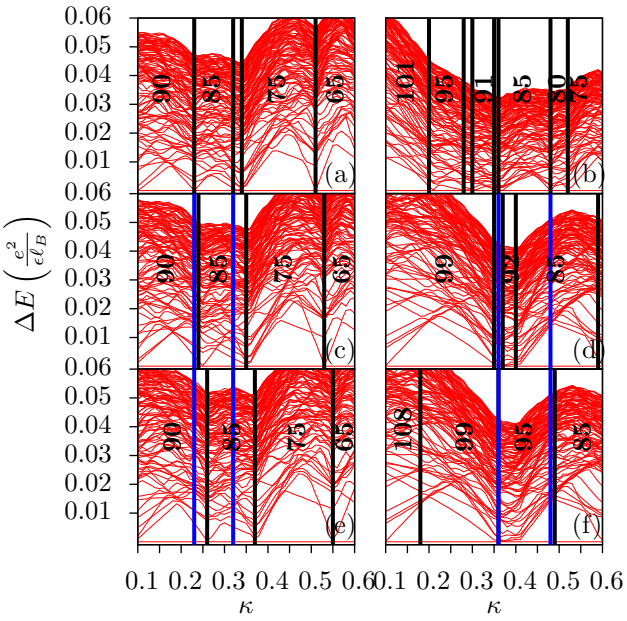

FIG. 5. The 100 lowest energy levels of 10 particles in 18 states for $d = 1.2\ell_B$ with $w = 0\ell_B$ (left) and $w = 1\ell_B$l (right). The individual graphs relate to different U for the Gaussian tip potential of Eq. (8) with $\sigma \simeq 4$: (a),(b) No Gaussian tip potential, (c) $U = 0.01e^2/\epsilon\ell_B$, (d) $U = 0.05e^2/\epsilon\ell_B$, (e) $U = 0.02e^2/\epsilon\ell_B$, (f) $U = 0.1e^2/\epsilon\ell_B$. The locations of the phase transitions are highlighted by the vertical black bars and the κ range of the $U = 0$ $M = 85$ phase is bordered by blue in all plots.

that the overlap with the Pfaffian at fixed d decreases with increasing κ, as was observed in Ref. 26.

The anti-Pfaffian, the $M = 101$ region in Fig. 2, favors a smoother edge (large d) and strong magnetic fields (small κ). Thus, the anti-Pfaffian prefers weaker confinement than the Pfaffian state. This is the opposite of observations in Ref. 26 where the Pfaffian appears at $\kappa < \kappa_c(w)$ and transitions to the anti-Pfaffian when $\kappa > \kappa_c(w)$. The reversal of this behavior we observe here is a result of the interaction with the neutralizing background as the overlap with the anti-Pfaffian increases sharply with increasing κ, as shown in Fig. 3b. As the neutralizing background plays an important role in experimental settings, we believe that the transition observed experimentally in Ref. 38 is of the type we observe here.

Another noticeable feature is the $M = 45$ collapsed state. This region represents the collapse of the 2DEG to the center of the disk where the state is supported only by degeneracy pressure. This is a result of LL mixing and the neutralizing disk potential overcoming Coulomb repulsion entirely. Comparing our 10 electron calculations to calculations with the 8 electrons, shown Fig. 4, we see that this state is pushed to higher κ by the introduction of new compressible stripe states as the particle number increases.

We may also compare the Pfaffian and anti-Pfaffian regions of the 8 and 10 particle results. Doing so, we see that the anti-Pfaffian does not stabilize. This is attributed to finite size (small number of particles) effects. The limited system size prevents the anti-Pfaffian from stabilizing due to the limited number of states available at the edge. The Pfaffian region, on the other hand, shrinks as more compressible states appear in the 10 electron case. This, however does not mean that the Pfaffian state vanishes in the thermodynamic limit, because the strength of the overlap integral increases with increasing particle number, so that the Pfaffian region does not appear to destabilize with increasing particle number and many of its features are enhanced.

These key points distinguish our results for the 2D phase diagram from what is expected from Ref. 32. When the finite thickness of the well is introduced, the potentially incompressible states appear much stronger than in the 2D case, as is expected[28–30], with the incompressible states occurring at much lower d than in the 2D case. However, several features of both cases do not differ that dramatically, particularly the presence of the $M = 101$ region and the $M = 85$ region separated by a series of compressible stripe states, with the $M = 85$ region having a strong overlap with the Pfaffian throughout.

In order to examine the phase transitions, we take a cut across the phase diagram at fixed $d = 1.2\ell_B$ and perform a higher resolution sweep of the LL mixing strength as shown in Fig. 5a,b. A striking difference between the pure 2D case, when $w = 0$, and the finite width confinement, $w = 1\ell_B$, immediately becomes apparent as we

look at the energy gaps. In the system with $w = 0\ell_B$, all ground states develop an energy gap, as we move away from the phase transition. For $w = 1\ell_B$, the energy gaps for the stripe phases have closed and only the candidate incompressible states continue to possess an energy gap. In the $M = 101$ region, we take this and the rapid increase of the overlap integral as κ and d increase shown in Fig. 3b as an indication of this region belonging to the same class as the anti-Pfaffian.

The results in Fig. 5 also show that the energy gaps of the incompressible states close linearly with κ. This behavior has also been identified experimentally in Ref. 33, where several samples were studied at different LL mixing strength. Additionally, the experimental results favored the MR Pfaffian in the strong LL mixing case, in agreement with our phase diagram. The experiment also indicates less sensitivity to d than we observe, but relatively stronger sensitivity to d is a finite size effect because the range of d we explore is on the same scale as the size of our model system, while the d in the experimental setup is significantly smaller than the system size studied experimentally.

IV. QUASIHOLES

With the phase diagram established, we now explore the effects of introducing a quasihole at the center of the system. Such a quasihole excitation can be introduced by depopulating the center of the disk with the potential

$$\hat{H}_U = U \sum_m \exp \frac{-m^2}{2\sigma^2} a_m^\dagger a_m, \tag{8}$$

which is equivalent to applying a repulsive Gaussian tip to the center of the disk. U is the strength and σ is the width of the potential, which correlates with the size of the quasihole. The results are shown for Fig. 5c-f, alternating between $w = 0\ell_B$ and $w = 1\ell_B$.

As we increase the strength of the tip potential, for $w = 0\ell_B$, the $M = 85$ phase begins to be displaced by the neighboring $M = 90$ phase associated with the formation of a charge $e/4$ quasihole[39]. In previous work in the disk configuration, with no account of LL mixing, such quasihole states were introduced using a tip potential with a size $\sigma \simeq 3$, but in order to introduce a quasihole excitation here, with LL mixing present, we must increase the size of the Gaussian tip to $\sigma \simeq 4$, which is in agreement with Ref. 34. For $w = 1\ell_B$, we are no longer able to introduce a single quasihole excitation, but we may introduce a pair of quasiholes at much stronger strengths. This may be an indication of pairing in the ground state as the two-quasihole state does not change the boundary conditions and leaves the edge structure unchanged.

In order to understand the increase in size of the charge $e/4$ quasihole, we consider the classical effects of introducing LL mixing. Adiabatically turning on LL mixing by increasing κ, is formally equivalent to decreasing the magnetic field. Then a small amount of negative charge is transported from the center of the disk to the edge by this process and the equilibrium state of the same angular momentum M has more charge located on the edge. As the charge $e/4$ quasiholes are effectively a center of rotation, a similar effect should occur, increasing the size of the region of depleted charge. Thus, the inclusion of LL mixing leads to an increase in quasihole size.

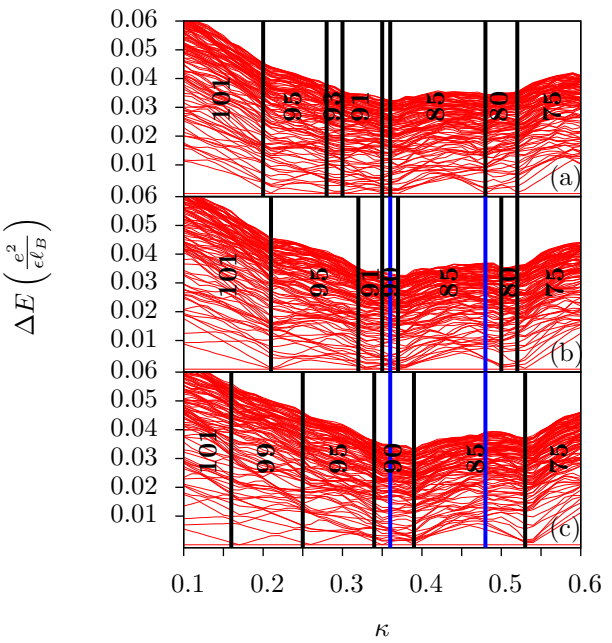

FIG. 6. The same as in Fig. 5, but only results for $w = 1\ell_B$ are shown with a Gaussian tip potential with $\sigma \simeq 4.5$ and (a) $U = 0$, (b) $U = 0.01e^2/\epsilon\ell_B$, (c) $U = 0.02e^2/\epsilon\ell_B$. The increased tip size creates and expands a phase with an $M = 90$ ground state with a charge $e/4$ quasihole isolated at the center of the disk.

When introducing finite thickness effects, the confining potential generated by the neutralizing background is weakened. As a result, stronger LL mixing is required to overcome the Coulomb repulsion and realize the $M = 85$ Pfaffian state. Since this is then an even smaller magnetic field than in the $w = 0\ell_B$ case, more charge will be located on the edge of the disk when we include finite thickness. Similarly, introducing a quasihole should push more charge away from the center of rotation. Therefore, the charge $e/4$ quasiholes should be larger when we include finite thickness effects. Thus, when σ in Eq. (8) is increased, we expect that a single quasihole excitation in the $w = 1\ell_B$ system will be produced as U is increased.

The results for $\sigma \simeq 4.5$ and $w = 1\ell_B$ are shown in Fig. 6. Turning on U with this larger Gaussian tip, we can see that a new phase appears between the $M = 95$ and $M = 85$ Pfaffian state. The increase of 5 units of angular momentum is the angular momentum associated with a single quasihole excitation and we see that the $M = 90$ state displaces the $M = 85$ Pfaffian state as U is increased, just like what we see in the $w = 0\ell_B$ case.

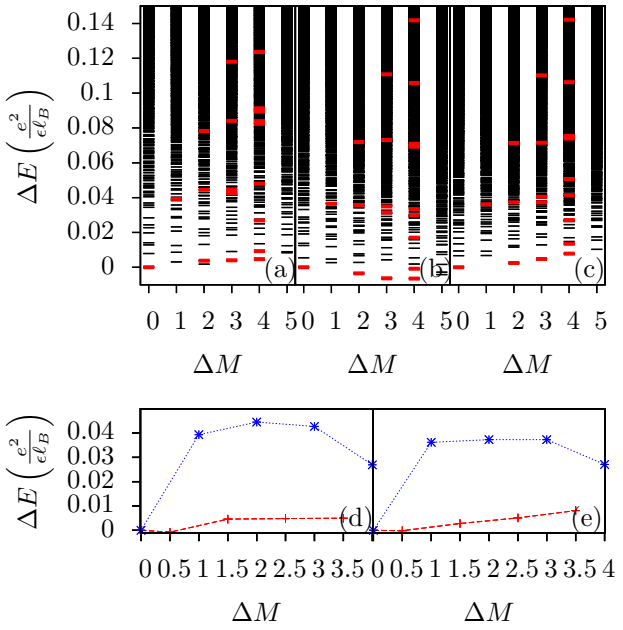

FIG. 7. (a) The spectrum of 10 particles in 22 states for $d = 1.2\ell_B$, $\kappa = 0.3$, and $w = 0\ell_B$ with the edge states highlighted in red. (b),(c) The same as (a), but for $w = 1\ell_B$ at $\kappa = 0.4$ and $\kappa = 0.5$, respectively. (d),(e) The energies of the Fermi (red) and Bose (blue) edge modes as a function of angular momentum with $w = 0\ell_B$ and $w = 1\ell_B$, respectively.

Therefore, we see that both finite thickness effects and Landau level mixing leads to a larger quasihole size.

V. EDGE STATES

We now focus on the edge states of the $M = 85$ Pfaffian region. A signature of the Pfaffian state is the presence of two edge modes, a neutral Bose mode, which carries the quasiparticle charge around the edge, and a neutral Fermi mode, which arises from pair-breaking excitations and carries the quasiparticle statistics[40]. For the phase diagrams in Fig. 2, we use a smaller set of basis states in order to limit the effects of edge reconstruction and limit the influence of the edge states[31,32]. At present, however, we wish to emphasize the edge characteristics and so we increase the size of our single particle state space from 18 states to 22 states in the 10 particle case. This has the additional effect of driving the Pfaffian state to higher LL mixing strengths as the smaller state space acted as an artificial confining potential.

In order to determine the edge states, we calculate the overlap integrals between these states and the zero energy expansions and pair-breaking excitations of the ideal three-body Hamiltonian[7,8,40]. For the single particle Bose modes and the Fermi modes, the overlap integrals are shown in Table I for the results in Fig. 7(b). For edge excitations that are a combination of Bose and Fermi modes, the overlap integrals are weaker and we rely upon the energies and the overlap integrals to determine these states. We find similar overlap integrals for the other energy spectra shown in Fig. 7.

ΔM	$\lvert\langle\psi_M\rvert\psi_{\text{edge}}\rangle\rvert^2$
0	0.36
1_B	0.33
2_B	0.18
2_F	0.31
3_B	0.12
3_F	0.36
4_B	0.14
4_F	0.23
4_F	0.2

TABLE I. The overlaps of the edge states at various ΔM consisting of either a single Bose mode or two Fermi edge modes for $w = 1\ell_B$, $d = 1.2\ell_B$ and $\kappa = 0.4$. The Bose modes at a given angular momentum are indicated by m_B and the Fermi modes by m_F. For the first Bose mode and the Fermi modes, we see that the overlap integral is close to that of the ground state with the Pfaffian (indicated by $\Delta M = 0$), but falling as we look at higher ΔM.

We first look at the case where $d = 1.2\ell_B, \kappa = 0.3$ and $w = 0\ell_B$ in Fig. 7a. In the spectrum, we identify two clear branches of edge modes: an upper and a lower branch. The lower branch represents the purely Fermi edge modes, which are largely separated from the bulk, though there is still some mixing at $\Delta M = 2$. The upper branch is well mixed with the bulk and consists of the Bose edge modes and the mixed edge modes. Recent results suggest that as we are looking at $d > 0.5\ell_B$, we should see edge reconstruction[35]. Instead, we find that LL mixing has overcome edge reconstruction and kept the system in the $M = 85$ region. This is further illustrated in the $w = 1\ell_B$ case which we describe below.

For the $w = 1\ell_B$ system, we examine $\kappa = 0.4$ in Fig. 7b. At this κ, the state has undergone edge reconstruction and some of the Fermi edge modes lie below the $M = 85$ state. As we increase LL mixing and look at the $\kappa = 0.5$ case, we see that the edge reconstruction is overcome by the effects of LL mixing and $M = 85$ is recovered as the ground state. Thus our choice of a truncated state space has reduced the κ at which the incompressible states occur. Additionally, we see that the Fermi branch is even more well separated from the bulk states than in the system with $w = 0\ell_B$.

With the edge states identified, we calculate the single mode energies. Comparing the results in Fig. 7d,e for the $w = 0\ell_B$ and $w = 1\ell_B$, respectively, we see that the dispersion of the Fermi edge mode becomes significantly more linear as finite thickness is introduced. From this spectrum, we calculate the dispersion relation, which gives the velocities and allows us to calculate the quasiparticle coherence length[41]. We find $L_\phi \simeq 1.93\mu$m and $L_\phi \simeq 2.82\mu$m for $w = 0\ell_B$ and $w = 1\ell_B$ respectively.

These values are lower than previous results[32], though we examine a larger separation d. As larger separations lead to a smoother edge potential, which lowers the coherence length, we expect to find even smaller coherence lengths at experimentally relevant values.

VI. DISCUSSION

In conclusion, our simulations of the $\nu = 5/2$ FQHE on a disk of neutralizing charge in the presence of LL mixing and inclusion of finite thickness effect by an infinite rectangular well potential confining the 2DEG give three primary results. First, we observe a possible phase transition from the anti-Pfaffian state to the Pfaffian state as the interaction strength κ is increased. This dependence on κ is the opposite of that obtained in systems with spherical geometry[26], and the difference arises from the inclusion of interactions with the neutralizing background. At fixed separation d, κ acts to bend the phases so that they occur at larger d than they originally appear, and the incompressible regions expand as w is increased. We also find that only the Moore-Read and anti-Pfaffian states continue to possess energy gaps at finite well width, while the gaps for the compressible stripe states close, which is similar to experimental observations[33]. Second, for the charge $e/4$ quasiholes, we found that the quasihole size necessarily increases as a result of the decreasing characteristic magnetic field strength for increasing κ and also depends upon the strength of the confining background potential. Additionally, the quasihole size is also influenced by the well thickness as a result of the weaker confinement offered by the neutralizing background. Third, the LL mixing is essential for the realization of the Pfaffian state in the expanded state space, as edge reconstruction destroys the signatures of the Pfaffian state for relatively small d otherwise. The edge structure of the Pfaffian is drastically improved when both κ and w increase.

From our results, we have evidence that various device parameters may play a role in determining which incompressible state is achieved in the sample. For example, in our phase diagram, varying the separation between the neutralizing background and the 2DEG can change whether the Pfaffian or the anti-Pfaffian is realized at fixed κ. When experimental results are considered, we begin to see a case for various sample dependent parameters controlling which incompressible ground state is realized. As an example, we highlight the results of Ref. 42, which shows a tunnel conductance consistent with the abelian Halperin 331 state[43], and those of Ref. 14, which show a non-abelian signature under variation of flux through the sample.

Our results in combination with these experimental results lead us to conclude that there exist several incompressible states that may be realized in the $\nu = 5/2$ FQHE. With advances in these studies, it should be possible to gain the ability to engineer samples which achieve a specific ground state. As an example of this, it will be of interest to explore a more complex treatment of sublevel mixing where partial occupation of different sublevels could produce the two populations necessary for the Halperin 331 state.

ACKNOWLEDGMENTS

This work was supported by the U.S. Department of Energy, Office of Basic Energy Sciences, Division of Materials Sciences and Engineering under Award DE-SC0010544.

[1] R. Willett, J. P. Eisenstein, H. L. Stormer, D. C. Tsui, A. C. Gossard, and J. H. English, Phys. Rev. Lett. **59**, 1776 (1987).
[2] W. Pan, R. R. Du, H. L. Stormer, D. C. Tsui, L. N. Pfeiffer, K. W. Baldwin, and K. W. West, Phys. Rev. Lett. **83**, 820 (1999).
[3] R. B. Laughlin, Phys. Rev. Lett. **50**, 1395 (1983).
[4] J. K. Jain, Phys. Rev. Lett. **63**, 199 (1989).
[5] V. W. Scarola, K. Park and J. K. Jain, Nature **406**, 863 (2000).
[6] G. Moore and N. Read, Nucl. Phys. B **360**, 362 (1991).
[7] M. Greiter, X.-G. Wen, and F. Wilczek, Phys. Rev. Lett. **66**, 3205 (1991).
[8] M. Greiter, X.-G. Wen, and F. Wilczek, Nucl. Phys. B **374**, 567 (1992).
[9] M. Levin, B. I. Halperin, and B. Rosenow, Phys. Rev. Lett. **99**, 236806 (2007).
[10] S.-S. Lee, S. Ryu, C. Nayak, and M. P. A. Fisher, Phys. Rev. Lett. **99**. 236807 (2007).
[11] V. Gurarie and C. Nayak, Nucl. Phys. B **506**, 685 (1997).
[12] D. A. Ivanov, Phys. Rev. Lett. **86**, 268 (2001).
[13] Y. Tserkovnyak and S. H. Simon, Phys. Rev. Lett. **90**, 016802 (2003).
[14] R. L. Willett, L. N. Pfeiffer, and K. W. West, PNAS **106**, 8853 (2009).
[15] S. Das Sarma, M. Freedman, and C. Nayak, Phys. Rev. Lett. **94**, 166802 (2005).
[16] P. Bonderson, A. Kitaev, and K. Shtengel, Phys. Rev. Lett. **96**, 016803, 2006).
[17] M. R. Peterson, K. Park, and S. Das Sarma, Phys. Rev. Lett. **101**, 156803 (2008).
[18] W. Bishara and C. Nayak, Phys. Rev. B **80**, 121302 (2009).
[19] S. H. Simon and E. H. Rezayi, Phys. Rev. B **87**, 155426 (2013).
[20] M. R. Peterson and C. Nayak, Phys. Rev. B **87**, 245129 (2013).
[21] I. Sodemann and A. H. MacDonald, Phys. Rev. B **87**, 245425 (2013).
[22] R. E. Wooten, J. H. Macek, and J. J. Quinn, Phys. Rev. B **88**, 155421 (2013).

[23] A. Wojs, C. Toke, and J. K. Jain, Phys. Rev. Lett. **105**, 096802 (2010).
[24] E. H. Rezayi and S. H. Simon, Phys. Rev. Lett. **106**, 116801 (2011).
[25] Z. Papic, F. D. M. Haldane, and E. H. Rezayi, Phys. Rev. Lett. **109**, 266806 (2012).
[26] K. Pakrouski, M. R. Peterson, Th. Jolicoeur, V. W. Scarola, C. Nayak, and M. Troyer, Phys. Rev. X **5**, 021004 (2015).
[27] M. P. Zaletel, R. S. K. Mong, F. Pollmann, and E. H. Rezayi, Phys. Rev. B **91**, 045115 (2015).
[28] M. R. Peterson, Th. Jolicoeur, and S. Das Sarma, Phys. Rev. Lett. **101**, 016807 (2008).
[29] M. R. Peterson, Th. Jolicoeur, and S. Das Sarma, Phys. Rev. B **78**, 155308 (2008).
[30] Y. Liu, D. Kamburov, M. Shayegan, L. N. Pfeiffer, K. W. West, and K. W. Baldwin, Phys. Rev. Lett. **107**, 176805 (2011).
[31] X. Wan, E. H. Rezayi, and K. Yang, Phys. Rev. B **68**, 125307 (2003).
[32] X. Wan, Z.-X. Hu, E. H. Rezayi, and K. Yang, Phys. Rev. B **77**, 165316 (2008).
[33] N. Samkharadze, J. D. Watson, G. Gardner, M. J. Manfra, L. N. Pfeiffer, K. W. West, and G. A. Csáthy, Phys. Rev. B **84**, 121305 (2011).
[34] S. L. Sondhi and S. A. Kivelson, Phys. Rev. B **46**, 13319 (1992).
[35] Y. Zhang, Y.-H. Wu, J. A. Hutasoit, and J. K. Jain, Phys. Rev. B **90**, 165104 (2014).
[36] F. D. M. Haldane, Phys. Rev. Lett. **51**, 605 (1983).
[37] S. H. Simon, E. H. Rezayi, and N. R. Cooper, Phys. Rev. B **75**, 195306 (2007).
[38] N. Samkharadze, L. N. Pfeiffer, K. W. West, and G. A. Csathy, aRxiv:1302.1444 (unpublished).
[39] C. Nayak and F. Wilczek, Nucl. Phys. B **479**, 529 (1996).
[40] M. Milovanovic and N. Read, Phys. Rev. B **53**, 13559 (1996).
[41] W. Bishara and C. Nayak, Phys. Rev. B **77**, 165302 (2008).
[42] X. Lin, C. Dillard, M. A. Kastner, L. N. Pfeiffer, and K. W. West, Phys. Rev. B **85**, 165321 (2012).
[43] B. I. Halperin, Helv. Phys. Acta. **56**, 75 (1983).